Including Diffuse Multipath Parameters in MIMO Channel Models

Nicolai Czink[1,2], Andreas Richter[3], Ernst Bonek[1], Jukka-Pekka Nuutinen[4], Juha Ylitalo[4]
[1]Institut für Nachrichtentechnik und Hochfrequenztechnik, Technische Universität Wien, Austria
[2]Forschungszentrum Telekommunikation Wien (ftw.), Vienna, Austria
[3]Signal Processing Laboratory, University of Helsinki, Finland
[4]Elektrobit, Finland
nicolai.czink@nt.tuwien.ac.at

***Abstract*— Recent findings suggest to split the impulse response of the radio channel into discrete paths and the "diffuse multipath" (DMP). This diffuse part can be described by an exponentially decaying power delay profile.**

This paper shows how to improve current radio channel models using the DMP concept. From MIMO channel measurements, we find that the DMP parameters are strongly correlated with the parameters of the discrete paths. This holds for various (indoor) environments. We provide a simple way to model the statistics of the DMP parameters.

Finally, we include the DMP concept in a novel MIMO model, the Random-Cluster model. We find that including DMP significantly improves the model fit in terms of mutual information and channel diversity.

***Keywords*—MIMO channel; diffuse multipath; geometry-based stochastic channel models**

I. Introduction

Current advanced MIMO channel models use the concept of describing the radio channel by multiple, clustered but *discrete* paths (e.g. line-of-sight paths, or paths from specular reflections). This approach raises two questions: (i) How many paths need to be included in the model? (ii) How to model signal components that are not discrete?

Recently, Richter [1] observed from MIMO channel measurements that, after estimating and subtracting discrete paths, a residual with a specific structure, the *diffuse multipath* (DMP), remains (due to e.g. reverberation of the room or distributed scattering). The DMP is sufficiently described by only three parameters, which reduces the complexity of the modelling significantly.

Using the DMP in modelling provides answers to both questions raised above. The complexity can be significantly reduced by taking only dominant paths into account, while the DMP describes the non-discrete signal components in the radio channel.

Contribution Although there are already papers describing the parameters of the DMP [1]–[4], no information about how to include this knowledge into current MIMO channel models was given, yet. In order to improve these models, we provide a simple statistical, yet accurate model for the parameters of the DMP. We show that the parameters describing the power-delay profile of the DMP are correlated with parameters used in current MIMO channel models to characterize *discrete* paths.

Organisation Section II describes the DMP phenomenon, outlines the estimation of the diffuse-multipath parameters, and provides a model for generating new DMP responses. In Section III, we provide a simple way to obtain the diffuse-multipath parameters from indoor MIMO channel measurements, and detail how to obtain new realisations of this model. Section IV validates the diffuse parameter model. Finally, Section V concludes the paper.

Part of this work was generously supported by Elektrobit Testing Ltd., as well as by the Austrian Kplus program.

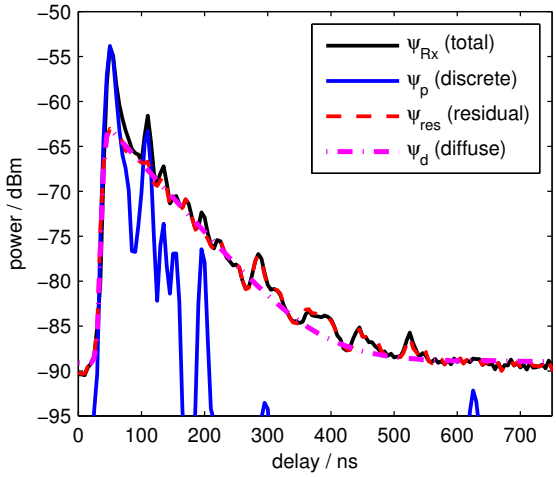

Fig. 1. Diffuse power

II. Diffuse Multipath

A. Description

The description of the DMP phenomenon has been observation-driven. Richter [1] found that, after subtracting a number of discrete paths from the channel impulse response, an exponentially decaying residual power delay profile (PDP) remains. Figure 1 shows an example, where the *total Rx* PDP (averaged over all N_t transmit and N_r receive antennas) $\psi_{\mathrm{Rx}}(\tau)$ (black line) can be approximated by estimated *discrete paths* with PDP $\psi_p(\tau)$ (blue), and a *residual* PDP $\psi_{\mathrm{res}}(\tau)$

(red). This residual PDP can be well approximated by an exponential PDP $\psi_d(\tau)$ describing the DMP (magenta).

Denoting the measured channel matrices with $\mathbf{H}_{\text{Rx}}(\tau)$ and channel matrices generated from discrete paths $\mathbf{H}_p(\tau)$, these PDPs can be calculated as

$$\psi_{\text{Rx}}(\tau) = \frac{1}{N_r N_t} \|\mathbf{H}_{\text{Rx}}(\tau)\|_{\text{F}}^2, \tag{1}$$

$$\psi_p(\tau) = \frac{1}{N_r N_t} \|\mathbf{H}_p(\tau)\|_{\text{F}}^2, \tag{2}$$

$$\psi_{\text{res}}(\tau) = \frac{1}{N_r N_t} \|\mathbf{H}_{\text{Rx}}(\tau) - \mathbf{H}_p(\tau)\|_{\text{F}}^2, \tag{3}$$

where $\|\cdot\|_{\text{F}}^2$ denotes the squared Frobenius matrix norm.

Following [2], the exponential DMP PDP approximating the residual PDP can be described by

$$\psi_d(\tau) = \begin{cases} 0, & \tau < \tau_d \\ \alpha_d/2, & \tau = \tau_d \\ \alpha_d e^{-B_d(\tau-\tau_d)}, & \tau > \tau_d, \end{cases} \tag{4}$$

where τ is the (sampled) delay, B_d is the decay factor, α_d denotes the maximum diffuse power, and τ_d is the (sampled) base delay. This equation was initially suggested by [5] to model the total PDP of a channel with small bandwidth. Since (4) has infinite bandwidth, we will show in the following subsections how to overcome this problem.

B. Model of diffuse multipath

To add DMP to an (already available) channel frequency response containing discrete paths $\mathbf{h}_p$, we use a noise-coloring filter in frequency domain. For this, we consider the Fourier transform of (4) ($\tau \Leftrightarrow \Delta\omega$)

$$\Psi(\Delta\omega) = \frac{\alpha_d}{B_d + \text{j}\Delta\omega} \text{e}^{-\text{j}\Delta\omega\tau_d}. \tag{5}$$

To implement a generator for the DMP, we introduce the normalised parameters $\beta_d = B_d/B$, $\tau_d' = \tau_d B/M$, and a sampled version of (5)

$$\boldsymbol{\kappa} = \frac{\alpha_1}{M} \left[\frac{1}{\beta_d} \quad \cdots \quad \frac{\text{e}^{-j2\pi(M-1)\tau_d'}}{\beta_d + j2\pi\frac{M-1}{M}} \right], \tag{6}$$

having M samples, and bandwidth B. Then, we use (6) to create a Toeplitz matrix and compute its Cholesky decomposition

$$\mathbf{R}_d = \text{toep}\big(\boldsymbol{\kappa}, \boldsymbol{\kappa}^{\text{H}}\big) = \mathbf{L}_{\text{d}} \mathbf{L}_{\text{d}}^{\text{H}}. \tag{7}$$

Finally, we obtain the *realisations* of the DMP according to

$$\mathbf{h}_d = \mathbf{L}_d \mathbf{w}, \tag{8}$$

where $\mathbf{w} \sim \mathcal{CN}(\mathbf{0}, \mathbf{I}) \in \mathbb{C}^{M\times 1}$ is a realisation of a circular, complex, i.i.d., zero-mean Gaussian distributed process. The sum of the impulse response of the discrete paths $\mathbf{h}_p$ and $\mathbf{h}_d$ result in a realisation of the channel in the frequency domain. If the number of frequencies M is large, it is reasonable to exploit the Toeplitz structure of (7) see [1] (pp. 152) for details.

Note that we currently consider the DMP to be spatially white. This means that independent, uncorrelated realisations of the DMP are added to the discrete channels. Since we are currently focussing on indoor modelling, this stipulation can be expected to be met, since diffuse power will most likely be scattered from all directions around the Tx and Rx. For outdoor cases, this stipulation has yet to be proven.

C. Estimation from residual PDP

In [2], the discrete paths and the exponential remainder were estimated jointly. In contrast to this approach, we first estimate the discrete components using the Initialisation-and-Search-Improved SAGE (ISIS) algorithm [6], and then estimate the parameters of the exponential remainder using a non-linear least squares parameter estimator.

Starting point is the (sampled) observation of the residual PDP $\psi_{\text{res}}(m\,\Delta\tau)$, with $\Delta\tau = 1/B$ denoting the intrinsic delay resolution, and $m = 1 \ldots M$ denoting the delay index. Collecting the DMP parameters in $\boldsymbol{\theta}_d = [\alpha_d\ \beta_d\ \tau_d']$, we can formulate the estimator as

$$\hat{\boldsymbol{\theta}}_d = \underset{\boldsymbol{\theta}_d}{\arg\min} \sum_{m=0}^{M-1} |\psi_{\text{res}}(m\,\Delta\tau) - \psi_d(m\,\Delta\tau, \boldsymbol{\theta}_d)|^2. \tag{9}$$

We can calculate the DMP PDP easily by first stacking the samples (delay-taps) as $\boldsymbol{\psi}_d = [\psi_d(0) \ldots \psi_d((M-1)\Delta\tau]^{\text{T}}$, and then using the Toeplitz matrix in (7) as

$$\boldsymbol{\psi}_d(\boldsymbol{\theta}_d) = \text{diag}[\mathcal{F}^{-1}\mathbf{R}_d(\boldsymbol{\theta}_d)\mathcal{F}], \tag{10}$$

with $\mathcal{F}$ denoting the Fourier-transform matrix and $\text{diag}[\cdot]$ denoting the vector of the diagonal elements of the matrix.

While values for the parameters were presented in [1]–[4], a way to incorporate this knowledge into current channel models was not provided. In the following we present a simple, straight-forward way to model the diffuse-multipath parameters.

III. Modelling diffuse-multipath parameters

In this section we will present an *observation-based model* for the DMP parameters. As a quite surprising result, we will show that the DMP parameters are significantly correlated with the PDP of the discrete components. We will detail how to obtain trustworthy diffuse-multipath parameters from a PDP of *discrete* components $\psi_p(\tau)$. To relate these parameters, we will introduce an observation-based model derived from MIMO indoor wideband measurements at 2.55 GHz.

A. Measurements

The measurements were carried out using an Elektrobit Propsound CS™ channel sounder at a carrier frequency of 2.45 GHz. We used semi-spherical antenna arrays at both link ends to be able to capture the full azimuthal domain around the transmitter and the receiver. The sounder and the antennas are described in more detail in [7].

For our evaluations in this paper we selected five scenarios with quite different propagation conditions. Three measurements were done in office rooms (see Figure 2a), and two measurements were conducted in big rooms, with and without line of sight (see Figure 2b). In all measurements the Tx was moved while the Rx was fixed, except for the "Stationary" environment, through which people moved occasionally.

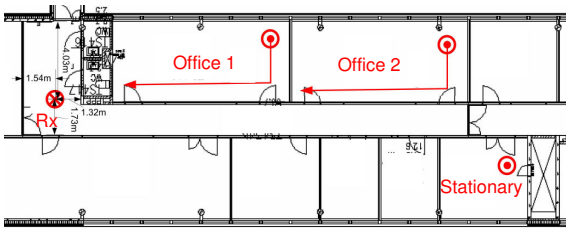

(b) Office scenarios

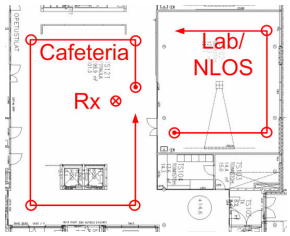

(a) Cafeteria (LOS) and Laboratory environment (NLOS)

Fig. 2. Measured scenarios: (a) Office rooms (room width $\sim$ 4 m), amply furnitured; (b) Left: Cafeteria (room length $\sim$ 9 m), metal tables and chairs, some people sitting at the tables; (b) Right: Laboratory environment, Rx in the Cafeteria. The red line shows the trajectory of the transmitter.

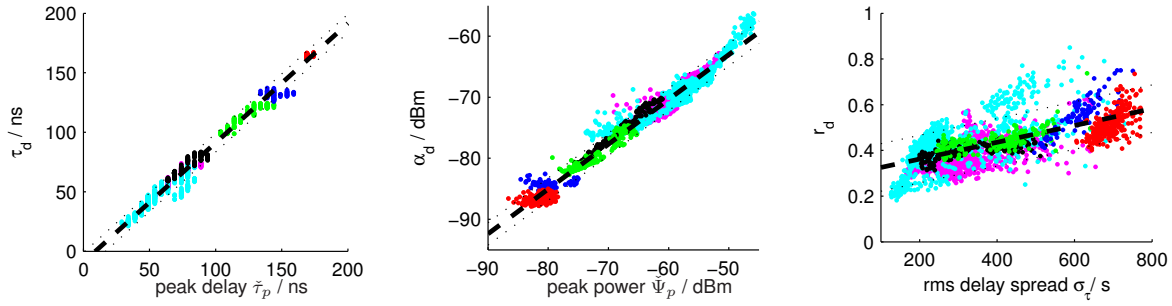

(a) (b) (c)

Fig. 3. Dependency of diffuse-multipath parameters. The black dashed line describes the linear regression curve, the dotted lines indicate the 3σ interval.

The measurements were post-processed using the ISIS SAGE algorithm [6] in order to estimate the discrete propagation paths for every snapshot. Subsequently, the residual PDP was calculated as in (3) from which we estimated the DMP parameters by using (9).

B. Observation

We relate the following observable quantities from the PDP of discrete components $\psi_p(\tau)$ to the diffuse-multipath parameters: (i) the base delay of the peak $\check{\tau}_p = \arg\max_\tau\{\psi_p(\tau)\}$, (ii) the peak power $\check{\psi}_p = \max\{\psi_p(\tau)\}$, and (iii) the rms delay spread σ_τ [8] of the total impulse response.

These parameters, related to the diffuse PDP, are shown in Figure 3. Scatter plots show the dependency of the DMP parameters to the quantities observed from the PDP of discrete components. Single snapshots are indicated by dots, where different colors indicate the different environments measured. In detail, the base delay of the diffuse components τ_d is correlated with the peak delay $\check{\tau}_p$ (Figure 3a). The diffuse-multipath peak parameter α_d is likewise correlated with the peak power $\check{\psi}_p$ (Figure 3b).

Finally, we use the ratio between the total diffuse power P_d and the total Rx power P_{Rx} as an auxiliary quantity $r_d = P_d/P_{\mathrm{Rx}}$, where P_d is given by

$$P_d = \int_0^\infty \psi_d(\tau)\mathrm{d}\tau = \frac{\alpha_d}{\beta_d}, \tag{11}$$

and similar definitions hold for the total Rx power and the total power of the discrete PDP, P_p.

Figure 3c reveals a positive correlation between the rms delay spread and the ratio of the diffuse power r_d.

Keeping the diffuse power ratio and the total power of the discrete components fixed, this leads to the power of the diffuse components as

$$P_d = \frac{r_d}{1-r_d}P_p. \tag{12}$$

A conclusion to be drawn from Figure 3 is that the correlations hold obviously for all environments investigated. Also, within a certain environment, represented by different dots of the same color, the correlations exist over large parameter ranges.

This conclusion might be surprising, but can be easily explained as follows:

The *base delay* of the DMP τ_d starts right with the first peak of the discrete paths, for two physical reasons: (i) local scattering around the terminal from scatterers that are within one delay bin (in our case corresponding to 3 m), (ii) scatterers that are close to the (quasi) line of sight. Both phenomena are very likely in indoor scenarios. The reason for some samples being below the regression line is that in some NLOS scenarios the strongest peak of the PDP comes later than the first contributions, i.e. the first *observable* discrete path has a larger delay than the first contribution to DMP.

The *diffuse peak power* α_d must be smaller than the discrete peak power, otherwise the path estimator would not be able to estimate any paths. But, when there is more power, hence better SNR, at the receiver, more dominant paths can be resolved, calling for a larger gap between the diffuse and discrete peak power. A more physical approach would be to correlate the diffuse peak power with the distance between Rx and Tx, where a correlation would be also very likely. But

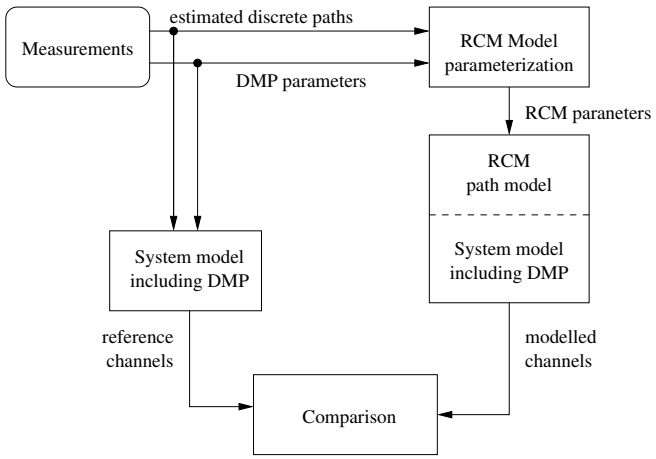

Fig. 4. Validation framework

since we do not have the actual distances available, we resort to the correlation with the discrete peak power.

Finally, the *power ratio of the DMP and the received power* is likely to depend on the rms delay spread of the total response for the same reasons as stated above. The longer the impulse response is, the stronger the contribution of the diffuse power will be. Note that the rms delay spread of the discrete components cannot be used here, they usually do not represent the delay spread of the actual impulse response of the channel correctly. Again, the physical distance between Tx and Rx may also have significant correlation with the diffuse power ratio.

C. Model of diffuse-multipath parameters

We model the DMP parameters in the measured environments by Gaussian probability distributions, where we define the mean and variance using a first-order polynomial fit (corresponding to linear regression) of the observation data

$$p_{\tau_d\left|\check{\tau}_p\right.} = \mathcal{N}(\check{\tau}_p - 9\,\mathrm{ns}, 27.0\,\mathrm{ns}^2), \tag{13}$$

$$p_{\alpha_d[\mathrm{dBm}]\left|\check{\psi}_p\right.} = \mathcal{N}(0.73 \cdot \check{\psi}_p - 26.3\,\mathrm{dBm}, 1.49\,\mathrm{dBm}^2) \tag{14}$$

$$p_{r_d\left|\sigma_\tau[\mu s]\right.} = \mathcal{N}(0.037 \cdot \sigma_\tau + 0.29, 0.0088) \tag{15}$$

where $\mathcal{N}(\mu, \sigma^2)$ denotes a realisation of a Gaussian random variable with mean μ and variance σ^2.

Realisations of the diffuse-multipath parameters can be obtained in the following way: By drawing realisations from the distributions (13) and (14), the base delay τ_d, and the peak power α_d are determined directly. The decay factor β_d is then determined by drawing a realisation of the diffuse power ratio from (15), obtaining the total diffuse power from (12), and calculating the decay factor by (11).

IV. Model validation

We validate the DMP model by a goodness-of-fit test. The general procedure is described in Figure 4. From the channel measurements we estimated discrete propagation paths and the DMP parameters.

Reference channels were generated from every measured snapshot by using a MIMO system model, considering 8×8 antennas and a bandwidth of $100\,\mathrm{MHz}$ at a carrier frequency of 2.55 GHz. After calculating the channel matrix from the discrete paths, the DMP was generated for each antenna link independently.

For the *modelled channels* we use the Random-Cluster Model (RCM) [9], a geometry-based stochastic MIMO channel model using multipath clusters to describe the discrete propagation paths of the channel. The RCM can be parameterized directly from measurements [7], which are used to describe the channel geometry by statistical means. Having modelled the discrete paths, the DMP parameters are obtained as described in Section III-C. Subsequently, the DMP is generated according to (8) for each link independently and added to the total channel transfer matrix.

In this paper, we present the validation for the Stationary Office environment (NLOS) and for the Cafeteria environment (LOS). Note that the RCM *path model* was parameterized by the measurements in the respective environments, but for the DMP model we used the parameters presented in Section III-C, obtained from a much larger set of measured data. For each scenario, we generated a number of 200 snapshots.

To assess the model fit to the reference channels we used the following metrics: (i) the CDF of the mutual information (MI) [10], and (ii) the channel diversity metric [11]. For intuitive comparison we use cumulative distribution functions representing the values of the metrics from different snapshots.

We compare the narrowband MI for a constant receive SNR of $10\,\mathrm{dB}$ in Figure 5 for both scenarios. We also show the impact of including the DMP in the model. Red colour indicate the modelled channels, blue color indicate the reference channels, while solid lines denote the inclusion of the DMP, and dashed lines denote the disregard of DMP.

Figure 5a shows the MI evaluated for the Stationary Office environment. First, we observe a significant difference between including the DMP in both the reference channels and in the model. The ergodic capacity changes considerably. We also find that the model fits the reference channels very well. A similar behaviour is noticed in the Cafeteria scenario in Figure 5b, with a significant change in outage capacity, while the ergodic capacity does not change too much, here. Again, the model fits the reference channels very well.

Since the MI curves indicated a strong difference in diversity, we also used the diversity metric [11] for comparing the channels. Again we compare the impact of including the DMP in the model. Figure 6a shows that neglecting DMP has a significant impact on diversity. In this scenario, the model creates slightly more diversity than available in the channel. The same holds true for the Cafeteria scenario in Figure 6b.

V. Conclusions

We presented a way to improve current MIMO radio channel models by including the diffuse multipath (DMP) concept. We found the surprising result that the DMP parameters are strongly correlated with the discrete channel response in the

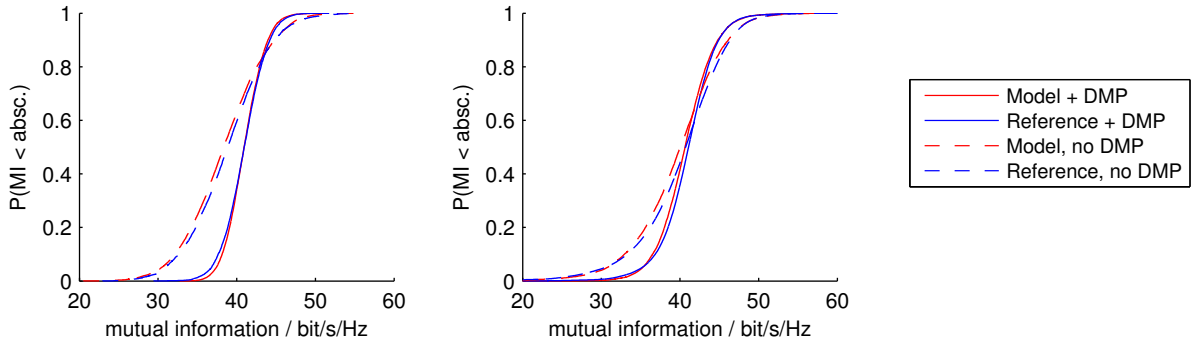

(a) Office (b) Cafeteria

Fig. 5. Mutual information

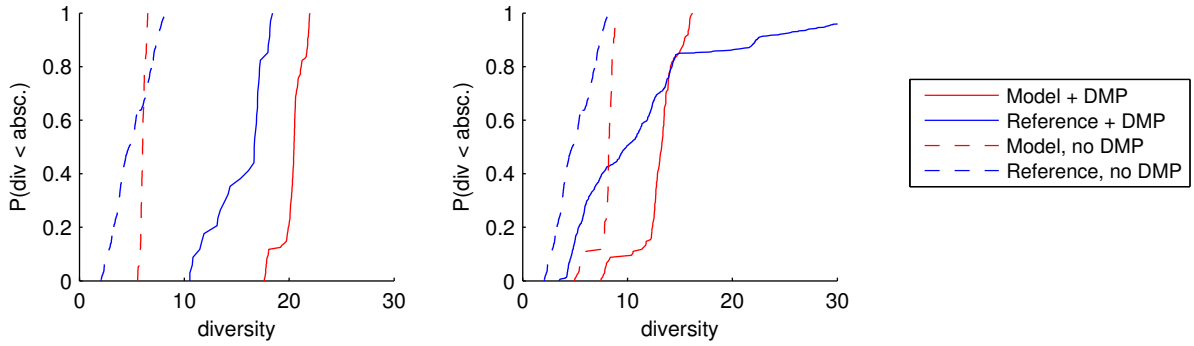

(a) Office (b) Cafeteria

Fig. 6. Diversity measure

measured indoor environments. The correlation is largely independent of the propagation environment, but strongly depends on the PDP of the discrete paths. The reason for this can be well explained by physical mechanisms, but a validation of the found parameters by other groups is still outstanding.

In a first approach we assumed the DMP to be spatially white. This is a good approximation for indoor scenarios, where one can expect diffuse power from all directions.

After evaluating the DMP parameters in a number of environments, we provided a simple model for the diffuse-multipath parameters and showed how to include the DMP into a novel MIMO channel model, the Random-Cluster Model. When neglecting DMP, both mutual information and channel diversity turn out too small in the model, but the fits between experiment and model become convincingly good when the DMP is included.

Even though this paper showed the correlations between discrete and diffuse parameters, it is anticipated that some parameters of the DMP depend on other basic physical properties of the MIMO channel, as well.

REFERENCES

[1] A. Richter, "Estimation of radio channel parameters: Models and algorithms," Ph.D. Dissertation, Technische Universität Ilmenau, Ilmenau, Germany, 2005.

[2] A. Richter, J. Salmi, and V. Koivunen, "An algorithm for estimation and tracking of distributed diffuse scattering in mobile radio channels," in *IEEE SPAWC*, Cannes, France, 2006.

[3] ——, "Distributed scattering in radio channels and its contribution to MIMO channel capacity," in *EUCAP 2006*, Nice, France, 2006.

[4] A. Richter, C. Schneider, M. Landmann, and R. Thomä, "Parameter estimation results of specular and dense multi-path components in micro-cell scenarios," in *WPMC 2004*, Abano Terme, Italy, Sept. 2004.

[5] V. Erceg, D. G. Michelson, S. S. Ghassemzadeh, L. J. Greenstein, A. Rustako, P. B. Guerlain, M. K. Dennison, R. S. Roman, D. J. Barnickel, S. C. Wang, and R. R.Miller, "A model for the multipath delay profile of fixed wireless channels," *IEEE JSAC*, vol. 17, no. 17, Mar. 1999.

[6] B. H. Fleury, X. Yin, P. Jourdan, and A. Stucki, "High-resolution channel parameter estimation for communication systems equipped with antenna arrays," *Proc. 13th IFAC Symposium on System Identification (SYSID 2003), Rotterdam, The Netherlands*, no. ISC-379, 2003.

[7] N. Czink, E. Bonek, L. Hentilä, J.-P. Nuutinen, and J. Ylitalo, "Cluster-based MIMO channel model parameters extracted from indoor time-variant measurements," in *IEEE GlobeCom 2006*, San Francisco, USA, Nov. 2006.

[8] B. H. Fleury, "First- and second-order characterization of direction dispersion and space selectivity in the radio channel," *IEEE Transactions on Information Theory*, vol. 46, no. 6, pp. 2027–2044, September 2000.

[9] N. Czink, E. Bonek, L. Hentilä, J.-P. Nuutinen, and J. Ylitalo, "A measurement-based random-cluster MIMO channel model," in *IEEE Antennas and Propagation Symposium 2007*, Honolulu, USA, June 2007.

[10] I. E. Telatar, "Capacity of multi-antenna gaussian channels," AT&T Bell Laboratories, Tech. Rep. BL0112170-950615-07TM, 1995.

[11] M.T. Ivrlac and J.A. Nossek, "Quantifying Diversity and Correlation of Rayleigh Fading MIMO Channels," in *IEEE International Symposium on Signal Processing and Information Technology, ISSPIT'03*, Darmstadt, Germany, December 2003.